A New Parameter to Assess Hydromechanical Effect in Single-hole Hydraulic Testing and Grouting

Å. Fransson[a], C.-F. Tsang[b], J. Rutqvist[b], G. Gustafson[a]

[a]*Chalmers University of Technology, Göteborg, Sweden*
[b]*Lawrence Berkeley National Laboratory, Berkeley, California, USA*

Abstract

Grouting or filling of the open voids in fractured rock is done by introducing a fluid, a grout, through boreholes under pressure. The grout may be either a Newtonian fluid or a Bingham fluid. The penetration of the grout and the resulting pressure profile may give rise to hydromechanical effects, which depends on factors such as the fracture aperture, pressure at the borehole and the rheological properties of the grout. In this paper, we postulate that a new parameter, Å, which is the integral of the fluid pressure change in the fracture plane, is an appropriate measure to describe the change in fracture aperture volume due to a change in effective stress. In many cases, analytic expressions are available to calculate pressure profiles for relevant input data and the Å parameter. The approach is verified against a fully coupled hydromechanical simulator for the case of a Newtonian fluid. Results of the verification exercise show that the new approach is reasonable and that the Å-parameter is a good measure for the fracture volume change: i.e., the larger the Å-parameter, the larger the fracture volume change, in an almost linear fashion. To demonstrate the application of the approach, short duration hydraulic tests and constant pressure grouting are studied. Concluded is that using analytic expressions for penetration lengths and pressure profiles to calculate the Å parameter provides a possibility to describe a complex situation and compare, discuss and weigh the impact of hydromechanical couplings for different alternatives. Further, the analyses identify an effect of high-pressure grouting, where uncontrolled grouting of larger fractures and insufficient (or less-than-expected) sealing of finer fractures is a potential result.

Keywords: Hydromechanical; Fractured rock; Hydraulic testing, Grouting

1. Introduction

Sealing of tunnels by grouting is a method commonly used to minimize inflow of water and to enhance the stability of the tunnel. Small inflows also decrease the risk of lowering the ground water level, which may influence the environment in a negative way. The science of grouting is interdisciplinary and requires understanding of geology, hydrology, rheology, chemistry, rock mechanics and grouting technology. This is the reason why the science of grouting is complex and in spite of great effort many questions have still to be solved.

This paper deals with grouting of fractured rock with associated hydraulic testing, both of which may give rise to rock deformation due to hydromechanical coupling. Discussions are in the context of grouting as a part of a tunnel excavation cycle and as an example, six different tunnel projects in Sweden and Norway were studied in [1] identifying that a grouting method could in general consist of five main activities: (1) drilling; (2) grouting; (3) waiting; (4) probe holes /

water loss measurements and; (5) re-grouting. For these projects, water loss measurements or outflow measurements were performed before and/or after grouting or not at all.

The main objectives of this paper are to:
- Link the areas of grouting and hydro-mechanical coupling.
- Introduce a new parameter, the Å-parameter to provide a possibility to describe a complex situation and compare, discuss and weigh the impact of hydromechanical couplings for different alternatives.
- Verify the approach numerically and give some grouting related examples.

Issues associated with sealing of tunnels by grouting may be divided into three main areas: geology and the characterisation of the rock mass; grouting materials; and grouting technology. These topics and related equations are treated below. Then, equations governing hydromechanical coupling in rock response to grouting are presented. Following this, the use of a new parameter, Å, as a measure of hydromechanical effect is introduced, and its applicability is verified against a fully coupled hydromechancial numerical code. Finally, results of a few example cases using the Å parameter approach are presented, before concluding the paper with some remarks.

2. Literature review

2.1. Characterisation of the rock mass

When considering geology and characterisation of the rock mass as input to optimizing grouting design, extensive research has been performed for several years in the area of nuclear waste management, see [2] and [3]. Further, descriptions of individual fractures based on their aperture distribution have been the topic of papers by, e.g., [4], [5] and [6]. However, a difficulty arises since direct investigations of these fractures cannot be performed during construction in rock and the only way to obtain data for a description is through indirect methods. Hydraulic (*in-situ*) measurements, [7] and [8], provide information on the geometry of the conductive features of the rock mass. One of the parameters obtained is referred to as transmissivity, which is the ability of the rock mass (or conductive features) to transmit water. Between parallel plates, transmissivity is related to the so-called hydraulic aperture, *b*, based on the "cubic law" [9]:

$$T = \frac{\rho g b^3}{12\mu} \tag{1}$$

where ρ is the density, g is the acceleration due to gravity and μ is the viscosity. For a discussion of various type of apertures, please see [10]. In [11] the logarithm of the aperture (described as the difference between the initial aperture at zero stress and the joint closure at very high stress) was plotted against the logarithm of specific flow (flow per unit head gradient, $Q/\Delta h$), which is proportional to *T*. If the cubic law applies, this should result in a line with the slope 3, see Equation 1.

To get an idea of what strategy to use before grouting a section of a tunnel, water loss measurements can be performed in the boreholes of the grouting fan, resulting in a number of Lugeon values ([12], [13] and [14]), which are calculated as follows: Lugeon value = water loss

in litres/(meter·minute·MPa). As commented by [15] a high frequency of fine joints may give the same Lugeon value as a single wide fracture, and, when grouting is considered, the wide fracture has a large grout intake and the finer joints may not be groutable at all. Naturally this also affects the obtained pressure profiles. Unfortunately, often little effort is put on actually performing an adequate characterisation for grouting purposes. The research work carried out in for example [16], [17] and [18] aims at increasing the understanding of how to interpret and evaluate hydraulic tests to get more information about apertures of individual features for this particular purpose. This is considered to be of great importance since the aperture influences both inflow of water and the penetration of grout.

2.2. Grouting materials and grouting technology

The main advances regarding grouting technology in the last 10 years are concerned with better registration and controlling of the grouting process. New computer technology has enabled the flow and pressure of the grout-mix to be continuously registered. The basic equipment and technology however remain the same, see e.g. [12] and [13]. Parallel to studies on characterisation, research on the spreading of grout (cement-based grout) has been conducted by, e.g. [19]. A smaller field experiment including both hydraulic characterisation and cement grouting has been performed in a pillar at Äspö Hard Rock Laboratory (Äspö HRL) in Sweden, see [20] and [21]. In [22] the same pillar was grouted using another grouting material, Silica sol. Due to a small fracture aperture, the penetration of cement grout was very limited and in [22] a different part of the same fracture was grouted. Further, [23] present a tunnel grouting experiment including geological investigations, design, and excavation of a 70-metre tunnel in Äspö HRL. During this experiment, hydraulic tests and continuous testing of the grout were performed. Prediction of groutability based on both grout properties and hydrogeological data is also treated in [24] and [25]. Further, numerical codes have been developed based on the jointed rock mass and the rheology of the grout mix [26] and its penetrability, [27] and [19].

An important difference between water (used in hydraulic tests) and grout is the rheology. Here water is referred to as a Newtonian fluid having the viscosity, μ_w, whereas cement grout being a particle suspension is commonly described as a Bingham fluid with the viscosity, μ_B, and yield strength, τ_0. In [27] the average velocity of a Newtonian fluid (e.g. water) in a horizontal channel is expressed:

$$\bar{U} = -\frac{b^2}{12\mu_w}\frac{dp}{dx} \tag{2}$$

whereas the average velocity of a Bingham fluid would be [27]

$$\bar{U} = -\frac{b^2}{12\mu_B}\frac{dp}{dx}\left(1 - 3\frac{Z_{gr}}{b} + 4\left(\frac{Z_{gr}}{b}\right)^3\right) \tag{3}$$

where $2Z_{gr}$ is the total thickness of a solid core given in terms of a yield strength parameter τ_0 as follows:

$$Z_{gr} = \min\left(\frac{\tau_0}{\left|\frac{dp}{dx}\right|}, \frac{b}{2} \right) \tag{4}$$

The solid core is formed around the centre of the fracture if the shear stress there is less than the shear strength. From Equations 3 and 4, the maximum penetration of a Bingham fluid is found when the fluid velocity is equal to zero and is given by

$$I_{max} = \frac{\Delta p b}{2\tau_0} \tag{5}$$

dependent on the pressure change or the pressure difference between grout and water, Δp, the aperture, b, and the yield strength, τ_0. In [25] the relationship between penetration of grout and time is described using the dimensionless parameters $I_D = I/I_{max}$ and $t_D = t/t_0$, see Appendix A.

2.3. Hydromechanical coupling

Both hydraulic testing and grouting may give rise to deformation due to hydromechanical coupling (see e.g. [28] and [29]) and as commented by [28] coupling of processes implies that one process affects the initiation and progress of another, so that the rock fracture behaviour cannot be predicted by considering each process independently. According to [28] hydrological processes include: (1) fluid flow; (2) tracer transport and; (3) transient pore fluid pressure changes (occur due to injection or pumping etc.). The mechanical processes include: (1) opening or closing; (2) shear; (3) joint propagation and; (4) fracturing at joint tips.

Hydromechanical response due to pressure changes was studied by, e.g., [30] and [31]. Both references deal with *in situ* testing, the first for hydraulic testing in a borehole and the second investigates the hydromechanical behaviour of a pressurized single fracture. A review of the role of hydromechanical coupling in fractured rock engineering is presented in [32]. Of interest from a hydraulic testing and grouting perspective would be what is described as a "fluid-to-solid coupling" occurring when a change in fluid pressure or fluid mass produces a change in the volume of the porous media. Further, defining effective normal stress as

$$\sigma_n' = \sigma_n - p \tag{6}$$

then, the fracture normal deformation may be expressed as

$$\Delta u_n = \frac{\Delta \sigma_n'}{k_n} \tag{7}$$

In these expressions, σ_n is the total normal stress, p is the fluid pressure and k_n is the fracture normal stiffness. The normal deformation is non-linear when a normal stress is applied. The rate of deformation is greatest at low values of normal stress. This has been described by e.g. [33]:

$$\sigma_n' = \frac{\Delta V}{V_m - \Delta V} \xi + \xi \tag{8}$$

where ξ is the seating pressure or the initial condition for measuring the normal deformation, ΔV, and V_m is the maximum possible normal closure at the seating pressure. Equation 8 above could also be expressed:

$$\Delta u_n = \frac{\sigma_{ni}'}{k_{ni}} \left(1 - \frac{\sigma_{ni}'}{\sigma_n'} \right) \tag{9}$$

where Δu_n is the fracture normal deformation and σ_{ni}' (ξ above) and k_{ni} are respectively the total normal stress and the fracture normal stiffness at an initial reference stage [30].

2.4. In situ hydromechanical properties of fractures

Aperture and fracture normal stiffness are key parameters for investigating hydromechanical effects during high-pressure water injection and grouting. At a typical fractured rock site, fractures may vary in characteristics and size and from minor tensile cracks to major shear fractures and shear zones. Major shear fractures open to water flow tend to dominate inflow into tunnels. For example [5] investigated the aperture distribution of a highly-conductive shear fault at the Äspö Hard Rock Laboratory, Sweden. The fault belong of a group of steep-dipping fracture zones, typically 10-30 m long, of a type found to be the most conductive in the area. The investigations showed that the fault was undulating by a shear slip of about 4 cm, creating large areas of open channels between mineral filled contacts. The average aperture of the fracture was about 2 mm (outside contact zones), whereas the contact area, defined as the area with aperture less than 0.1 mm covered about 40% of the total fracture area. At the other end of the spectrum are tensile cracks that may be connected and hydraulic conductive but generally having much smaller aperture. For example [30] measured *in situ* hydraulic apertures ranging from 8 to 22 μm using hydraulic injection tests on fractures located between 81 to 417 meters depth.

Fracture normal stiffness as well as coupled stress and flow properties have been measured routinely on laboratory samples over the past 20 years. However, there are only a few data existing on the *in situ* hydromechanical behavoir of fractures, and data from major fractures are rare. One rare example of an *in situ* hydromechanical investigation on a major fracture is the one conducted by [31], at a granitic fractured rock site in Southwest of Sweden. A horizontal fracture located at about 70 meters depth and extending about 10 m was investigated by hydraulic tests in seven subvertical boreholes, which intersected the fracture a few meters apart. Alm's [31] field tests indicated that the *in situ* fracture normal stiffness at the seven locations ranged between 2 to10 GPa/m, whereas hydraulic conducting aperture ranged between 100 to 250 μm. The lowest values of normal stiffness (about 2 GPa/m) was measured at the location of the largest fracture aperture (about 250 μm). The range of normal stiffness values obtained by Alm is in agreement with *in situ* measurements by [34], who determined a fracture normal stiffness of 2.5 GPa/m with an aperture of 300 μm for a major sheared fracture located at about 250 m depth. Moreover, recent *in situ* measurements of major shear fractures by [35] indicated that an *in situ* fracture normal stiffness ranging between 8 to 50 GPa/m for apertures ranging 50 to 100 μm. For smaller fractures, likely representing mated tensile joints, [30] estimated the *in situ* fracture stiffness

ranging from 30 to 1100 GPa/m for fracture apertures ranging from 8 to 22 microns. Note that these values of fracture stiffness and apertures are different from those frequently measured in laboratory on small-scale drill core samples. In such experiments the aperture usually ranges from a few to tens of microns with a fracture normal stiffness orders of magnitude higher than those measured *in situ* [32]. However, the aforementioned *in situ* experiments were conducted using hydraulic injection tests, in which increasing the fluid pressure within the fracture opens the fracture. In so-called hydraulic jacking tests, fluid is injected from a borehole into a single fracture at step-wise increasing pressure and fracture opening is monitored from the step-wise increasing flow rate (e.g. [30]). Thus, hydraulic jacking tests involves opening (unloading) of fractures under increasing fluid pressure, that is, the same processes at the fracture opening that could take place during grouting. Therefore, apertures and fracture normal stiffness determined from such *in situ* experiments are well representative for the hydromechanical behaviour during grouting.

3. Conceptualization and definition of Å-parameter

Sealing of tunnels include several different activities. Considered here are: hydraulic testing (water loss tests and natural inflow); grouting with Newtonian fluids and; grouting with Bingham fluids. These activities may result in a change in aperture due to pressure changes in the fracture. A pressure – aperture response of a fracture is due to interrelated effects of the form: $\Delta p \rightarrow \Delta \sigma' \rightarrow \Delta u \rightarrow \Delta b$. In other words, a change in pressure affects the effective stress, which causes a mechanical deformation, which in turn leads to a change in the hydraulic aperture [36].

In the present paper, only fracture normal deformation is considered. In order to investigate and compare the pressure profiles and resulting deformations and changes in transmissivity (if any) for single-hole hydraulic tests and grouting both "shallow" tunnels where the normal stress is assumed to be small compared to the change in pressure, and "deep" tunnels where the normal stress is assumed being comparatively large are considered in the discussion. Here, Δp is the change in pressure at the borehole. Since the pressure profile is not unique but dependent upon fracture aperture (and its spatial variation in general), rheological properties of the grout, etc. we postulate that a new parameter, Å, which is defined as the integral of the change in fluid pressure, $\Delta p(r)$, in the fracture plane from the radius of the well to infinity, is an appropriate measure to describe the change in effective stress that gives rise to mechanical deformation.

$$\int_{r_w}^{\infty} 2\pi r \cdot \sigma_n' dr - \int_{r_w}^{\infty} 2\pi r \cdot \sigma_{ni}' dr = \int_{r_w}^{\infty} 2\pi r \cdot \Delta p(r) dr = Å \qquad (10)$$

In contrast to this equation, the expression $\sigma_n' = \sigma_{ni}' + \Delta P_w \cdot C$ was used in reference [30] and the factor C was introduced assuming that an "average" change of fluid pressure in the fracture area around the borehole (wellbore) is proportional to the change of well pressure. Using an integral, Equation 10 allows the consideration of potentially different types of variation in pressure in the fracture plane around the borehole.

Further, we postulate that the fracture volume change integrated over the fracture plane is proportional to the integral of the effective stress change, i.e. the Å parameter (*cf*. Equation 7).

As an illustration of the calculation of the Å-parameter, we show here the case of Newtonian fluid (water), which can be done analytically. The pressure profile can be derived based on the cubic law (Equation 1) and Thiem´s formula, e.g. [7]:

$$\Delta h = \frac{Q}{2\pi T} \ln \frac{r}{R} \tag{11}$$

where R is set to the radial extension of the drawdown cone, r_e:

$$r_e = \sqrt{\frac{2.25Tt}{S}} \tag{12}$$

The storage coefficient, S, is estimated based on an expression, found by regression using Äspö Hard Rock Laboratory data [37]:

$$S = 0.00922 \cdot T^{0.785} \tag{13}$$

Resulting in the following expression of the Å-parameter:

$$\mathring{A} = \int_{r_w}^{r_e} 2\pi r \cdot \Delta p \, dr = \frac{12Q\mu_N}{b^3} \left(\frac{r_w^2 \ln(r_w/r_e)}{2} - \frac{r_w^2}{4} + \frac{r_e^2}{4} \right) \tag{14}$$

The expressions used for calculation of the Å-parameter for the Newtonian (Silica sol) and the Bingham fluids are presented in Appendix A.

4. Verification of Å-parameter approach against results of a fully coupled HM simulator for the case of Newtonian fluids

Modelling was performed using a finite element numerical code, ROCMAS ([38], [30] and [39]). The numerical model is used for coupled stress and fluid flow analysis of fractured rock masses and solves simultaneously two sets of finite-element equations: the static equilibrium force-displacement equation and the quasi-steady-state fluid flow equation. The numerical solution gives coupled stress and fluid pressure fields in the fractured medium.

To verify the Å-parameter approach for the case of a Newtonian fluid (water), we assume an axisymmetric model, 10 by 10 meters. A fracture is located on the bottom of the model and extends the entire 10 meters radius, and a borehole is assumed to intersect the joint perpendicularly. However, the results are not expected to be significantly different if the intersection deviates moderately from perpendicular. By symmetry, half of the fracture is included in the model. We have used a linear stiffness option of the ROCMAS code and input data are presented in Table 1. The fracture normal stiffness values were selected range reasonable values that have been observed from various *in situ* hydraulic jacking measurements as reviewed in Section 2.4. A fracture normal stiffness of 4 GPa/m would represent a very shallow major fracture and the 400 GPa/m would represent deep-sited fracture exposed to a higher normal stress. A rock matrix Young's modulus of 70 GPa, and a matrix Poisson's ratio of 0.25 were assumed, which are reasonable values for granitic rock.

The analysis was performed using the following steps: (1) a constant pressure boundary was imposed at 3, 5 or 7 meters was assumed; (2) steady state analyses with an extension of 3, 5 or 7 meters were made to obtain a profile for pressure change, $dp(r)$, without allowing for hydromechanical coupling (i.e., no change in aperture), and (3) a profile of aperture change, $db(r)$ from numerical simulation including hydromechanical coupling, and (4) plotting of the integrated pressure change (the Å-parameter) from step (2) and the integrated volume change from step (3).

Fig. 1 shows the Å-parameter versus the fracture volume change for three different cases, with (a) fracture normal stiffness of 400 GPa/m; (b) fracture normal stiffness of 40 GPa/m; and (c) fracture normal stiffness of 4 GPa/m. Points along the lines corresponds to pressure profiles for different injection times, except for case (b), where additionally (the points on the circle-dashed line in Fig. 1) those for varied injection pressures were also calculated.

The figure clearly shows that the Å-parameter is a good measure for the fracture volume change: i.e., the larger the Å-parameter, the larger the fracture volume change, in an almost linear fashion. This is independent of whether the pressure profile is induced by larger injection time, or by higher injection pressure, which means that it is independent of the detailed pressure profile. Thus at least for Newtonian fluids, which is the case studied in these verification simulations, we can use the Å-parameter as a comparative measure to evaluate the impact of hydromechanically induced fracture volume changes for alternative grouting procedures. We postulate that the Å-parameter can equally be used for Bingham fluids in this way.

Let us consider the lines in Fig. 1 again. Note that they are almost linear. The early parts of these curves have slopes that are representative of "system stiffness", which is a function of fracture normal stiffness k_{nf} and matrix stiffness k_{nm} (the latter depending on E, the Young's modulus of the matrix). A discussion of system stiffness is given in [30]. In general these parameters cannot be obtained easily in the field, especially during the stage of construction and grouting. In our approach, we assume that they are the same for a given fracture in an in situ environment, and then use the Å-parameter as a relative measure to assess hydromechanical effects for alternative strategy for grouting the fracture.

5. Use of Å-parameter in example applications

The fracture-borehole configuration consists of one borehole intersecting two fractures with constant apertures b_1 and b_2, see Fig. 2. The scenario is injecting grouting fluids into the borehole for grouting the two fractures. Analyses are made using analytical calculations, and pressure profiles are determined for both Newtonian and Bingham fluids, based on the work of [22], [25] and [40]. These references derive and describe the relationship between penetration of the grout and the injection time using the dimensionless parameters $I_D = I/I_{max}$ and $t_D = t/t_0$. This approach assumes non-deformable fractures, non-compressible fluids and that the pressure change in the groundwater ahead of the front of the grouts (both Newtonian and Bingham grouts) can be neglected due to the distance from the borehole and the viscosity of the grouts being larger than that of water. These grout properties are summarized in Table 2, to be compared with water properties needed for analyzing water loss measurements.

The following three cases are studied: (1) *One individual fracture* varying: the aperture; the pressure at the borehole; the duration of hydraulic testing and grouting; and the fluid properties

(Newtonian or Bingham). Further, a comparison of fluid pressure profiles for *two fractures with a smaller and a larger aperture* (50 µm and 250 µm, respectively) is made. Both fractures are assumed to be subjected to either (2) the *same normal stress and loading history* or (3) *different normal stresses*, i.e. located near a "shallow" or "deep" tunnel.

5.1. Results

Table 3 presents results of injection pressure, injection volume, penetration distance and Å-parameter for an individual fracture at different injection pressures, different duration, and different fluid properties.

The different columns in the table represent: the hydraulic aperture, *b*, of a non-deformed fracture; the pressure change e.g. the difference between the grouting pressure at the borehole and the water pressure ($\Delta p = p_g - p_w$); and the duration of grouting or hydraulic testing. *I* is the penetration length of the grouts and the volume, *V*, is estimated based on the non-deformed fracture aperture and the penetration of the grout (minus the radius of the borehole). The percentage presented is based on simultaneous grouting of a 250 µm fracture and a 50 µm fracture without considering deformation, i.e. the percentage of the total volume found in each of the two fractures. *Å* is defined as the integral of the change in fluid pressure and the *Å-ratio* is estimated using the underlined 250 µm fracture as a basis for comparison. Table 4 presents the results for assumed water loss measurements.

5.2. Discussions of effects of injection pressure and grout penetration without mechanical deformation: one individual fracture

Radial fluid pressure profiles are presented in Fig. 3 for the two fractures using a constant pressure change at the borehole, Δp, of 0.4 MPa, during a 5-minute water loss measurement (NW in Fig. 3), and using a pressure change, Δp, of 2 MPa during a 20-minute grouting with a Newtonian fluid (NS in Fig. 3) and a Bingham fluid (B in Fig. 3).

The pressures along the profiles are presented based on different values of the radius where $r \leq I(t)$, which is the penetration length obtained for a given injection duration, t. Here, silica sol represents the Newtonian fluid, NS, and a cement grout represents the Bingham fluid, B. For the 250µm fracture and Δp: 2 MPa at the borehole, the grout take is low enough (250L, Table 3, below) as compared with a typical volume stop criterion of 50-100 litres per meter borehole (assuming the boreholes are between 10-20 meters). The penetration length (18 m) is too large since the borehole bottom distance is commonly between 2-4 meters. The penetration of the Newtonian fluid (Silica sol) is larger than for the Bingham fluid (cement grout) due to the yield strength and the higher viscosity of the Bingham fluid.

Based on these pressure profiles, less than half of the pressure at the borehole remains when the radius is larger than 20% of the penetration length. Further, the average pressure is about 10-15% of the pressure change at the borehole, *Δp*. This pressure is found at a radial distance of approximately 50-60% of the penetration length. Based on the shape of the pressure profiles, the Bingham fluid have less steep profiles and are less peaked than those for the Newtonian fluids; this is reflected in the somewhat higher average pressure. For longer durations, the shape of the Bingham fluid pressure profile continues to change and the shape at the maximum penetration,

I_{max}, is seen in Fig. 3. As commented based on a similar approach by [15], the extension of the pressurized surface will be limited and the average pressure acting on it can be estimated to be about 1/3 of the grouting pressure applied.

5.3. Discussion of effects of mechanical deformation on fracture grouting

[30] and [39] discussed in general the pressure and fracture opening that they are uneven over the fracture plane during injection and the fracture opens gradually as a function of the effective stress. In our approach we use an integral of the fluid pressure change from the radius of the well to infinity, the Å-parameter, as an appropriate measure to describe the change in effective stress that gives rise to mechanical deformation. Table 3 presents this Å-parameter for an individual fracture at different injection pressures, different duration, and different fluid properties. The ratios in the last column are used to see what situation is most likely to deform a fracture. The result from the 250µm fracture has been used as a basis for comparisons. In contrast, the water loss measurements (with water properties) are performed at a lower pressure and for shorter duration than grouting but even so the lower viscosity gives as a result a larger radius of influence, see Table 4. Consequently, the water loss test reflects the properties over a larger area than the grout but near-borehole effects will dominate in both cases. However the hydraulic aperture is likely to change only to a limited extent over this area, due to pressure commonly being small compared to the overburden.

5.3.1. Fractures subjected to the same normal stress and loading history
Let us assume that two fractures (e.g. 250µm and 50µm) have the same size and the same normal stress and loading history, and that the two fractures are intersected by the same borehole and are grouted by the same constant pressure for the same duration. For laminar flow, which is considered here, the resulting fluid pressure change in the 250 µm fracture compared with the 50 µm fracture will be slightly larger at a small radius and significantly larger for a large radius. This is reasonable since a smaller aperture has a larger flow resistance resulting in a larger gradient. For comparisons of the pressure profiles, the ratios of the fluid pressure integrals (Å-parameter) for different apertures and durations are presented, see Table 3.

The result from the 250µm fracture has been used as a basis for comparisons. According to these calculations, the ratio of Å-parameters for the 50µm fracture compared to the 250µm fracture would be 0.05. This is due to the fracture area subjected to pressure being much larger for the larger fracture. Based on [39] this should be of importance since a fluid penetrates into a fracture and opens it by the force of the fluid pressure inside the fracture. Assuming that the fracture having a larger aperture is also larger in size is not unlikely if it has a natural inflow and is a part of the main conductive system. This may result in a lower stiffness compared to a fracture of smaller size (and aperture). Consequently, the 250µm fracture is more likely to have a larger volume increase since it has a fluid pressure acting on a larger area as well as a lower stiffness.

When using high pressure grouting, the aim is to open the fractures to allow grouting of otherwise non-groutable fractures or part of fractures. According to [29] the reason for high pressure grouting is that low inflows (down to 1-2 L/min/100 m) have to be achieved. Increasing the grouting pressure would result in a larger penetration length even for a 50µm fracture. The reasoning goes as follows. From Equation 1, the transmissivity of a 250µm and a 50µm fracture would be approximately $1 \cdot 10^{-5}$ and $8 \cdot 10^{-8}$ m^2/s, respectively. At a hydraulic head (here, dh) of 10 meters the inflow would be 6 L/min for the large fracture and 0.05 L/min for the smaller one

(assuming Q≈T·dh). Increasing the hydraulic head to 350 meters would result in inflows of 205 and 1.6 L/min respectively. Having to control inflows down to 1-2 L/min/100 meters of tunnel, it would be sufficient with 20 fractures of 50µm aperture to reach this limit at a hydraulic head of 10 meters. For a deep tunnel, one small fracture would be enough. Consequently, sealing of both large and small aperture fractures is important to reach low inflows. However, the combination of a larger fracture that is more likely to deform (allowing more grout to enter) and a volume stop criteria would allow a shorter grouting time and possibly the final penetration length for the 50µm fracture would be approximately the same or maybe even shorter. As illustrated by Table 3, the grout volume for one 250µm fracture is 250 L at a pressure change of 2 MPa for 20 minutes and more than 500 L for a pressure change of 6 MPa for only 10 minutes. Adding to this a likely deformation of the 250µm fracture compared to the 50µm fracture makes it very difficult to know at what time or at what grout volume to stop the grouting for sealing of the smaller fractures. As presented in Table 3, 99% of the grout ends up in the larger fracture already before any deformation has occurred.

Since the relative penetration, I/I_{max}, is not a function of the aperture, [40] and [25], the penetration process for constant pressure grouting has the same time-scale for all fractures with different apertures intersected by a borehole. This means that the grout have reached the same percentage of its maximum penetration length in all fractures at a certain time. The fractures with the smallest aperture have the shortest maximum penetration. Considering this, the largest fluid pressure influence would always be seen for the largest aperture fracture which would therefore be more likely to deform when comparing larger apertures to smaller. Based on the discussion above, when both large and small aperture fractures are present along a borehole, only increasing the pressure may not solve the problem of sealing the smaller fractures. In case of small aperture fractures only, slight deformation may help to increase the fracture filling without risking too large spreading of the grout.

5.3.2. Fractures subjected to different normal stresses: "shallow" or "deep" tunnel
Since the fracture normal deformation is non-linear, [33] and [41], the rate of deformation being the greatest at low values of normal stress, there will be a difference in behaviour for a fracture subjected to a small normal stress e.g. by a "shallow" tunnel and a fracture subjected to a large normal stress e.g. by a "deep" tunnel. By approximating the overburden pressure to be 0.025 MPa per meter of depth. A shallow tunnel (e.g. 10 meters below ground) would have an approximate overburden pressure of 0.25 MPa whereas a deep tunnel (e.g. 450 meters, as in the Äspö HRL case, see [23]) would have an overburden pressure of approximately 11 MPa. For a shallow tunnel, deformation is likely to occur at a larger rate due to low normal stress, but the change in fluid pressure for different fracture apertures will still be in agreement with the discussion above.

For a natural inflow test similar fluid pressure profiles as for the 50µm and 250µm fracture could be calculated with the difference that the natural flow measurement gives a pressure drawdown and a possible decrease in aperture as a result, see example in [38]. The decrease in fluid pressure around the borehole would increase the effective stress resulting in a decreased aperture in the vicinity of the borehole that would limit the inflow and influence the estimated hydraulic aperture, see [42]. This changed aperture close to the borehole being smaller than the aperture b_0 at distance r_1, $b_1 < b_0$, may result in choking the inflow. Based on the rate of deformation being smaller at high values of normal stress, the natural water flow measurement is likely to give

smaller deformations at a large depth going from an already large to an even larger effective stress.

6. Concluding remarks

This paper deals with single hole hydraulic testing and grouting from a hydromechanical perspective. Radial pressure profiles based on analytical calculations without deformation are used in a new integral parameter Å that can be used to assess the hydromechanical effects and their implication on grouting efficiency under pressure.

Earlier, the virgin normal stress and the pressure at the well multiplied by a factor have been used to estimate an effective stress for a fracture. Here, the Å-parameter, which is postulated to measure the fracture volume increase, is used to see what situation is most likely to deform a fracture. Since the Å parameter can be calculated from analytic or semi-analytic expressions of penetration lengths and pressure profiles based on relevant input data, the approach gives a possibility to describe and assess a complex situation.

Initially, a verification of the Å parameter approach against results of a fully coupled hydromechanical simulator was made. For the case of a Newtonian fluid the study shows that the approach is reasonable and that the Å-parameter is a good measure for the fracture volume change: i.e., the larger the Å-parameter, the larger the fracture volume change, in an almost linear fashion.

Comparing a 250µm fracture to a 50µm fracture, when both are grouted at the same time, the ratio of the pressure integrals (Å-parameters) for the 50µm fracture compared to the 250µm fracture would be 0.05. This means that the 250µm fracture will open by a relatively larger volume upon pressurization as compared to the 50µm fracture. As presented here, 99% of the grout ends up in the larger of the two fractures already before any deformation has occurred. An increased pressure may result in a larger penetration length for both fractures but it is very difficult to know at what time or grout volume to stop the grouting for a better sealing of the smaller fractures. A normal volume stop criterion may actually result in a shorter penetration and smaller grout volume in the smaller-aperture fracture, due to the largest fracture deforming and taking more grout. Therefore, when both large and small aperture fractures are present along a borehole, only increasing the grouting pressure without increasing the grout stop volume may not solve the problem of sealing the smallest fractures. This is in agreement with a similar approach presented in [15]. A practical consequence presented by the author, which is also supported by this paper and the Å-parameter approach, is that "any grouting stage will fill mostly, or at least to a greater distance, only the main not already grouted joints, while the thinner ones will have to be grouted later on." An additional important remark by [15] is the possible closing of the thinner joints due to the expansion of the main joints. Thus, the effect of high-pressure grouting includes the risk of uncontrolled grouting of larger fractures and insufficient sealing of finer fractures. In case of small aperture fractures only, slight deformation may help to increase the fracture filling without risking too large a spreading of the grout.

A water loss measurement (injection test) as well as the grouting itself may result in local deformation (opening) due to the local increase in fluid pressure. However an increased aperture close to the borehole due to an injection test or grouting does not have to influence the predictions on the grouting to any larger extent, since the fluid pressure change is local and the

aperture further from the borehole is likely to remain unchanged still limiting the flow. Therefore the lower pressure used for the water loss measurement (injection) is not likely to be a problem even when used for predictions. This lower pressure is in some way compensated by a larger radius of influence due to the lower viscosity. Even though the deformation due to hydraulic tests and grouting would differ, the hydraulic tests should be used to make a more informed choice concerning what type of grout or pressure to use, which means also that the initial non-deformed conditions are of importance.

The aperture estimated from hydraulic tests is more likely to deviate from the grouted aperture at a shallow depth than deep due to the larger deformation rate. Further, the difference is probably larger for natural water inflow measurements than water loss measurements (injection). This is due to the natural inflow resulting in a decrease in fluid pressure, an increase in effective stress and a possible decrease in aperture. A local decrease in aperture close to the borehole has a larger influence on the estimated hydraulic aperture, $b(Q/dh)$ than an increase [42]. At a larger depth with higher stress and a smaller deformation rate, this problem is likely to be smaller. Therefore, from a hydromechanical point of view, water loss measurements may be preferable (and also more natural) compared to inflow measurements for grouting predictions at shallow depths.

As a final conclusion, using analytic expressions for penetration lengths and pressure profiles to calculate the suggested Å parameter provides a possibility to describe a complex situation and compare, discuss and weigh the impact of hydromechanical couplings for different alternatives.

Acknowledgements

Appendix A: Calculation of Å-parameter for Newtonian and Bingham fluids

The Å-parameter is the integral of the change in fluid pressure over the fracture plane. To determine a pressure profile at a certain time, dimensionless analyses are used. For both Newtonian and Bingham fluids, a dimensionless penetration length, I_D, is determined as a function of a dimensionless time, t_D. Curves relating I_D and t_D are found in [22] for Newtonian fluids, and in [40] and [25] for Bingham fluids.

For the Newtonian fluid (Silica sol), the parameters, I_{DN} and t_{DN} are determined based on the following equations:

$$t_{0N} = \frac{12 \cdot 10^4 \, \mu_g r_w^2}{\Delta p b^2} \tag{A1}$$

$$I_{DN} = \frac{I_N}{100 r_w} \tag{A2}$$

$$t_{DN} = \frac{t}{t_{0N}} = \frac{I_D^2}{2} \cdot \ln(100 I_D) - \frac{I_D^4}{4} + 2.5 \cdot 10^{-5} \tag{A3}$$

A certain grouting time, t, results in a penetration length, I_N, which is utilized instead of the radial extension of the drawdown cone, r_e, to estimate the Å-parameter (Equation 14, main text). To estimate a flow, Q, the density of the Silica sol is set to 1200 kg/m³. Input data for calculations including viscosity, μ_g, pressure, Δp, yield strength, τ_0 (for Bingham fluid) and apertures, b are presented in Table 2. The radius of the borehole, r_w, is 0.028 m.

For the Bingham fluid, the total penetration length, I_{max}, influences the result. The following equations are used to estimate the dimensionless penetration length, I_{DB}, at a certain dimensionless time, t_{DB}:

$$t_{0B} = \frac{6 \mu_g \Delta p}{\tau_0^2} \tag{A4}$$

$$I_{max} = \frac{b \Delta p}{2 \tau_0} \tag{A5}$$

$$I_{DB} = \frac{I_B}{I_{max}} \tag{A6}$$

$$t_{DB} = \frac{t}{t_{0B}} \tag{A7}$$

$$\gamma = \frac{I_{max}}{r_w} \tag{A8}$$

Further, based on equations below (see [40]), the penetration length $I_B(t)$ is used to determine pressure profiles for Bingham fluids at time t. Different times are used since hydraulic tests and grouting are not always performed for the same durations. In this analysis a dimensionless radius, r´, is used.

$$r' = \frac{r}{r_w} \tag{A9}$$

$$I' = \frac{I}{r_w} \tag{A10}$$

$$Q' = \frac{2\mu_g Q}{\pi b^2 \tau_0 r_w} \tag{A11}$$

$$\frac{Q'}{r'} = \frac{2\mu_g Q}{\pi b^2 \tau_0 r} \tag{A12}$$

$$p' = \frac{\gamma(p - p_w)}{\Delta p} \tag{A13}$$

$$p'(r') = \gamma - Q' \cdot \left[\tilde{G}(Q') - \tilde{G}(Q'/r') \right] \qquad 1 \le r' \le 1 + I' \tag{A14}$$

$$\tilde{G}(q) = G(\tilde{s}(q)) \tag{A15}$$

Initially,

$$\tilde{s}(q) = \frac{1}{2\sqrt{1+q} \cdot \sin\left\{ \frac{1}{3} \cdot \arcsin\left[(1+q)^{-1.5} \right] \right\}} \tag{A16}$$

is calculated, q is Q', Q'/r' and $Q'/(1+I')$.

Further, these values are used in:

$$G(s) = \frac{4}{3} \cdot \ln(s-1) + \frac{1}{6} \cdot \ln(2s+1) - \frac{1}{s-1} - \frac{3s^3}{(2s+1)(s-1)^2} \tag{A17}$$

to yield $G(\tilde{s}(Q'))$, $G(\tilde{s}(Q'/r'))$ and $G(\tilde{s}(Q'/(1+I')))$.

The two first values are used in Equation A14 to determine $p'(r')$. The pressure above groundwater pressure at the dimensionless r' is given by $p'(r') \cdot \Delta p / \gamma$ (Equation A13).

Q' has to be chosen to fulfill the following condition:

$$\gamma = Q' \cdot \left[\tilde{G}(Q') - \tilde{G}\left(\frac{Q'}{1+I'} \right) \right] \tag{A18}$$

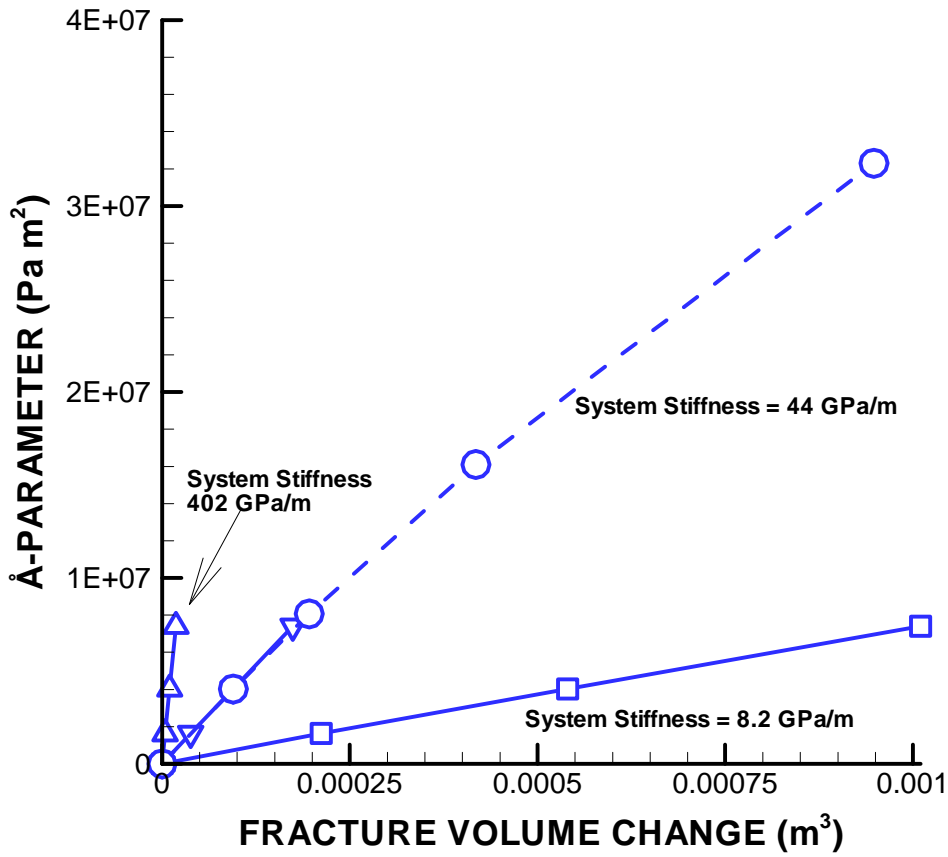The integral of the pressure profile over the area results in the Å-parameter.

Fig. 1. Integrated pressure (Å-parameter) versus fracture volume change for three different fracture normal stiffness: upward triangles for a fracture normal stiffness of 400 GPa/m; downward triangles and circles for a fracture normal stiffness of 40 GPa/m; and squares for a fracture normal stiffness of 4 GPa/m. Variation along the lines corresponds to different injection times, except for the circle-dashed line which corresponds to varied injection pressure for the case of fracture normal stiffness of 40 GPa/m.
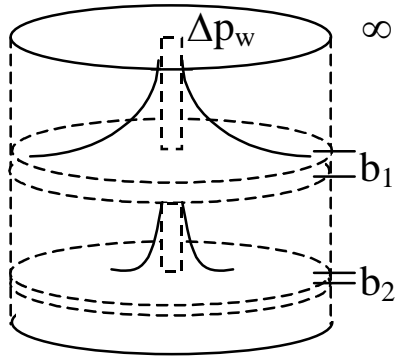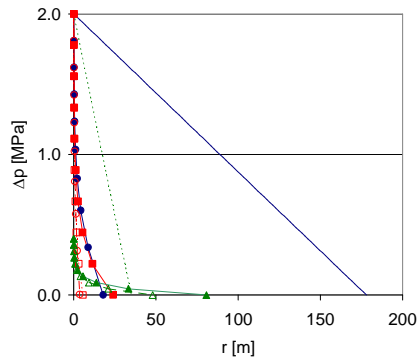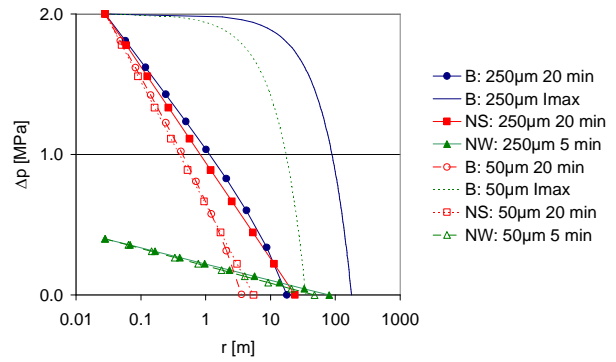
Fig. 2. Conceptual model of fracture-borehole configuration and pressure profiles. The pressure change at the well is Δp, the radial boundary is assumed to be at infinity

Fig. 3. Radial fluid pressure profiles for a 250 and 50 µm fracture using the pressure changes at the well of 0.4 MPa (water loss measurement for 5 minutes, NW in Figure) and 2 MPa (grouting with a Newtonian fluid, NS, and a Bingham fluid, B for 20 minutes). Also included I_{max} for the Bingham fluid. a) linear r, and b) logarithm of r.

Table 1
Input data for coupled numerical modelling.

Type of fluid	Newtonian
Fluid property, μ_w [Pa.s]	0.001
Well pressure change Δp [MPa above groundwater pressure]	0.5
"Penetration length", r_e [m]	3, 5, 7
Fracture aperture [μm]	250
Fracture normal stiffness, k_n [GPa/m]	4, 40, 400
Rock matrix modulus, E [GPa]	70
Rock matrix Poisson´s ratio, ν [-]	0.25

Table 2
Input data for calculations.

	Water loss measurements	Grouting	
Type of fluid	Newtonian	Newtonian	Bingham
Fluid properties	μ_w: 0.001 Pas	μ_g: 0.007 Pas	μ_g: 0.02 Pas τ_0: 1.4 Pa
Well pressure change Δp [MPa above groundwater pressure]	0.4	2, 6	2, 6
Duration [min]	5	10, 20	10, 20
Fracture configuration	2 fractures: 50µm & 250µm		

Table 3
Comparison of Å parameter and hydromechanical effects in a grouting procedure for two fractures intersected by the borehole.

	b [μm]	Δp [MPa]	Duration [min]	I [m]	Volume [m^3]	%	Å [Pa m^2]	Å-ratio*
a) Bingham fluid	250	2.0	20.0	17.9	0.250	99.2	2.3E+08	1.00
	50	2.0	20.0	3.6	0.002	0.8	1.1E+07	0.05
	250	6.0	10.0	26.8	0.564	99.2	1.2E+09	5.43
	50	6.0	10.0	5.4	0.005	0.8	6.2E+07	0.27
b) Newtonian fluid *"Silica sol"*	250	2.0	20.0	23.9	0.449	99.0	2.7E+08	1.16
	50	2.0	20.0	5.5	0.005	1.0	1.8E+07	0.08
	250	6.0	10.0	28.9	0.654	99.0	1.1E+09	4.91
	50	6.0	10.0	6.6	0.007	1.0	7.5E+07	0.32

* The underlined 250μm fracture is used as a basis for comparison.

Table 4
One fracture in water loss experiment: same pressure change, same duration, and same fluid properties, b: 50 µm and 250 µm.

	b [µm]	Δp [MPa]	Duration [min]	r_e [m]	Å [Pa m^2]	Å-ratio*
Newtonian fluid	250	0.4	5.0	80.6	5.1E+08	2.23
"water"	50	0.4	5.0	48.0	1.9E+08	0.84

* The underlined 250µm fracture is used as a basis for comparison.

References

[1] Dalmalm T. Choice of grouting method for jointed hard rock based on sealing time predictions. Ph.D. thesis, Royal Institute of Technology, Stockholm, 2004.

[2] SKB. Geoscientific programme for investigation and evaluation of sites for the deep repository. SKB, Technical Report TR-00-20, Stockholm, 2000.

[3] ENRESA. FEBEX project full-scale engineered barriers experiment for a deep geological repository for high level radioactive waste in crystalline host rock. ENRESA Publicación técnica 1/2000, Madrid, 2000.

[4] Gentier S, Billaux D, van Vliet L. Technical note: Laboratory testing of the voids of a fracture. Rock Mech Rock Eng 1989;89(22):149-157.

[5] Hakami E. Aperture distribution of rock fractures. Ph.D. thesis, Royal Institute of Technology, Stockholm, 1995.

[6] Zimmermann R W, Bodvarsson G S. Hydraulic conductivity of rock fractures. Trans Porous Media 1996;23:1-30.

[7] de Marsily G. Quantitative Hydrogeology. Groundwater hydrology for engineers. Academic Press, Inc., San Diego, 1986.

[8] Cooper H H, Jacob C E. A generalized graphical method for evaluating formation constants and summarizing well field history. Am Geophys Un Trans 1946;27:526-534.

[9] Snow D T. A parallel plate model of fractured permeable media. Ph.D. thesis, University of California, Berkeley, 1965.

[10] Tsang Y W. Usage of "Equivalent Apertures" for Rock Fractures as Derived From Hydraulic and Tracer Tests. Water Resour Res 1992;28:1451-1455.

[11] Witherspoon P A, Wang J S Y, Iwai K, Gale J E. Validity of cubic law for fluid in a deformable rock fracture. Water Resour Res 1980;16:1016-1024.

[12] Houlsby A C. Construction and design of cement grouting. John Wiley and Sons, Inc., New York, 1990.

[13] Kutzner C. Grouting of rock and soil. A. A. Balkema, Rotterdam, 1996.

[14] Palardy D, Ballivy G, Vrignaud J-P, Ballivy C. Injection of a ventilation tower of an underwater road tunnel using cement and chemical grouts. Grouting and Ground treatment, Proceedings of the third international conference, ASCE, Geotechnical special publication No 120, New Orleans, 2003.

[15] Lombardi G. Grouting of rock masses. Grouting and Ground treatment. Proceedings of the third international conference, ASCE, Geotechnical special publication No 120, New Orleans, 2003.

[16] Fransson Å. Characterisation of fractured rock for grouting using hydrogeological methods. Ph.D. thesis, Chalmers University of Technology, Göteborg, 2001.

[17] Fransson Å. Nonparametric method for transmissivity distributions along boreholes. Ground Wat 2002;40:201-204.

[18] Gustafson G, Fransson Å. The Use of the Pareto Distribution for Fracture Transmissivity Assessment. Hydrogeol J Issue: Online First DOI: 10.1007/s10040-005-0440-y, 2005.

[19] Eriksson M. Prediction of grout spread and sealing effect. A probabilistic approach. Ph.D. thesis, Royal Institute of Technology, Stockholm, 2002.

[20] Fransson Å. Characterisation of a fractured rock mass for a grouting field test. Tunnelling and Underground Space Technol 2001;16:331-339.

[21] Eriksson M. Grouting field experiment at the Äspö Hard Rock Laboratory. Tunnelling and Underground Space Technol 2002;17:287-293.

[22] Funehag J. Grouting of hard rock with gelling liquids, field and laboratory studies of Silica sol. Licentiate thesis, Chalmers University of Technology, Göteborg, 2005.

[23] Eriksson E, Fransson Å, Emmelin E. Grouting trials in hard jointed rock -investigation, design and execution. Proceedings of the16th International Conference on Soil Mechanics and Geotechnical Engineering, Osaka, 2005.

[24] Gustafson G, Stille H. Prediction of groutability from grout properties and hydrogeological data. Tunnelling and Underground Space Technol 1996;11:325-332.

[25] Gustafson G, Stille H. Stop Criteria for Cement Grouting. Felsbau 2005;3:62-68.

[26] Håkansson U. Rheology of fresh cement-based grouts. Ph.D. thesis, Royal Institute of Technology, Stockholm, 1993.

[27] Hässler L. Grouting of rock – simulation and classification. Ph.D. thesis, Royal Institute of Technology, Stockholm, 1991.

[28] Tsang C-F. Coupled hydromechanical-thermochemical processes in rock fractures. Rev of Geophys 1991;29:537-551.

[29] Barton N. The theory behind high pressure grouting – Part 1. Tunnels & Tunnelling Int 2004;September:28-30.

[30] Rutqvist J. Coupled stress-flow properties of rock joints from hydraulic field testing. Ph.D. thesis, Royal Institute of Technology, Stockholm, 1995.

[31] Alm P. Hydro-mechanical behaviour of a pressurized single fracture: an in-situ experiment. Ph.D. thesis, Chalmers University of Technology, Göteborg, 1999.

[32] Rutqvist J. Stephansson O. The role of hydromechanical coupling in fractured rock engineering. Hydrogeol J 2003;11:7-40.

[33] Goodman R E. The mechanical properties of joints. Proceedings of the 3rd Int. Congr. International Society of Rock Mechanics, Denver, Colorado. National Academy of Sciences, Washington, DC, 1974,I,127-140.

[34] Jung R. Hydraulic *in situ* investigation of an artificial fracture in the Falkenberg granite. Int J Rock Mech Min Sci Geomech Abstr 1989; 26:301-308

[35] Cappa F, Guglielmi Y, Rutqvist J, Tsang C-F, Thoraval A. Hydromechanical modeling of pulse tests that measure both fluid pressure and fracture-normal displacement at the Coaraze Laboratory site, France. Int J Rock Mech Min Sci 2006;43:1062-1082.

[36] Rutqvist J. Technical Note Determination of hydraulic normal stiffness of fractures in hard rock from well testing. Int J Rock Mech Min Sci Geomech Abstr 1995;32:513-523.

[37] Rhén I (ed), Gustafson G, Stanfors R, Wikberg P. Äspö HRL – Geoscientific evaluation 1997/5. Models based on site characterization 1986-1995. SKB, Technical Report 97-06, Stockholm, 1997.

[38] Noorishad J, Ayatollahi M S, Witherspoon P A. A finite-element method for coupled stress and fluid flow analysis in fractured rock masses. Int J Rock Mech Min Sci Geomech Abstr 1982;19:185-193.

[39] Rutqvist J, Tsang C-F, Stephansson O. Uncertainty in the maximum principal stress estimated from hydraulic fracturing measurements due to the presence of the induced fracture. Int J Rock Mech Min Sci Geomech Abstr 2000;37:107-120.

[40] Gustafson G, Claesson J. Steering parameters for rock grouting. Chalmer University of Technology, Göteborg, Sweden, submitted for publication, 2006.

[41] Bandis S, Lumsden A C, Barton N R. Fundamentals of rock joint deformation. Int J Rock Mech Min Sci Geomech Abstr 1983;20:249-268.

[42] Fransson Å. Grouting predictions based on hydraulic tests of short duration: analytical, numerical and experimental approaches. Licentiate thesis, Chalmers University of Technology, Göteborg, 1999.